Inorganic Chemistry

ARTICLE

pubs.acs.org/IC

Highly Luminescent Mixed-Metal Pt(II)/Ir(III) Complexes: Bis-Cyclometalation of 4,6-Diphenylpyrimidine As a Versatile Route to Rigid Multimetallic Assemblies

Valery N. Kozhevnikov,*[,†] Marcus C. Durrant,[†] and J. A. Gareth Williams*[,‡]

[†]School of Life Sciences, Northumbria University, Newcastle upon Tyne, NE1 8ST, U.K.

[‡]Department of Chemistry, Durham University, Durham, DH1 3LE, U.K.

Supporting Information

ABSTRACT: The proligand 4,6-di-(4-*tert*-butylphenyl)pyrimidine **LH_2** can undergo cycloplatination with K_2PtCl_4 at one of the two aryl rings to give, after treatment with sodium acetylacetonate, a mononuclear complex Pt($N^{\wedge}C$-LH)(acac) (denoted **Pt**). If an excess of K_2PtCl_4 is used, a dinuclear complex of the form [Pt(acac)]$_2${μ-($N^{\wedge}C$-L-$N^{\wedge}C$)} (**Pt_2**) is obtained instead, where the pyrimidine ring acts as a bridging unit. Alternatively, the mononuclear complex can undergo cyclometalation with a *different* metal ion. Thus, reaction of **Pt** with $IrCl_3 \cdot 3H_2O$ (2:1 ratio) leads, after treatment with sodium acetylacetonate, to an unprecedented mixed-metal complex of the form Ir{μ-($N^{\wedge}C$-L-$N^{\wedge}C$)Pt(acac)}$_2$(acac) (**Pt_2Ir**). The mononuclear iridium complex Ir($N^{\wedge}C$-LH)$_2$(acac) (**Ir**) has also been prepared for comparison. The UV−visible absorption and photoluminesence properties of the four complexes and of the proligand have been investigated. The complexes are all highly luminescent, with quantum yields of around 0.5 in solution at room temperature. The introduction of the additional metal centers is found to lead to a substantial red-shift in absorption and emission, with λ_{max} in the order **Pt** < **Pt_2** < **Ir** < **Pt_2Ir**. The trend is interpreted with the aid of electrochemical data and density functional theory calculations, which suggest that the red-shift is due primarily to a progressive stabilization of the lowest unoccupied molecular orbital (LUMO). The radiative decay constant is also increased. This versatile design strategy may offer a new approach for tuning and optimizing the luminescence properties of d-block metal complexes for contemporary applications.

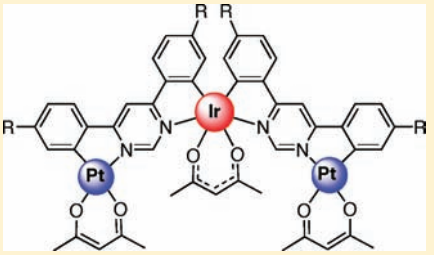

INTRODUCTION

Cyclometalated iridium(III) and platinum(II) complexes of 2-phenylpyridines and related ligands are often exceptionally good luminophores.[1−3] Current interest from academia and industry is driven, in particular, by their suitability for applications as phosphors in organic light-emitting diodes (OLEDs).[4] The success of such complexes in this field is mainly due to the spin−orbit coupling (SOC) effect induced by cyclometalated third row transition metal centers, which promotes efficient phosphorescence from the triplet state, allowing the harvesting of both singlet and triplet type excitons.[5] Meanwhile, other applications have emerged in parallel. For example, such complexes are attractive as the light-emitting units of sensory molecular systems whose emission is modulated upon binding of a target analyte,[6] or as intrinsically emissive probes that may localize in selected organelles within living cells.[7] They are also under investigation as potential photocatalysts for "water splitting" to generate hydrogen,[8] and as sensitizers of energy- and electron-transfer reactions, also relevant to the conversion of solar energy to electrical or chemical energy.[2,9,10]

The vast majority of cyclometalated Pt(II) and Ir(III) compounds studied to date incorporate a single metal center. Examples of luminescent *multinuclear* systems with cyclometallating ligands are less common, and mostly comprise two atoms of the same metal. In the case of Pt(II), for example, studies have generally been focused on the use of flexible or rigid linkers that bring together two square-planar, cyclometalated platinum units in a face-to-face manner, promoting Pt---Pt or ligand---ligand interactions and induction of lower-energy emission.[11] Meanwhile most of the examples involving iridium are represented by systems in which individual mononuclear metal complexes are connected either through an ancillary ligand or by a bridging ligand that acts as a partially insulating spacer. Examples include compounds that make use of *para*-phenylene-bridged bis-bipyridines to link two Ir(ppy)$_2$ units[12] or one such unit to a ruthenium(II) center;[10] related assemblies employing tridentate cyclometallating ligands in conjunction with bridging terpyridines;[13] and recent work with bridging acetylacetonate derivatives.[14] In such compounds, the metal centers retain properties that are similar to those of the isolated units, with the bridging ligand playing a relatively minor role.

Very few rigid systems in which two cyclometalated metal centers are connected by coordination to a common heterocyclic ring have been reported, and even fewer where the photophysical properties have been investigated. Hexa-azatriphenylene (HAT)

Received: April 6, 2011
Published: May 31, 2011

Scheme 1. Synthesis of Proligand LH_2 by Suzuki Cross-Coupling

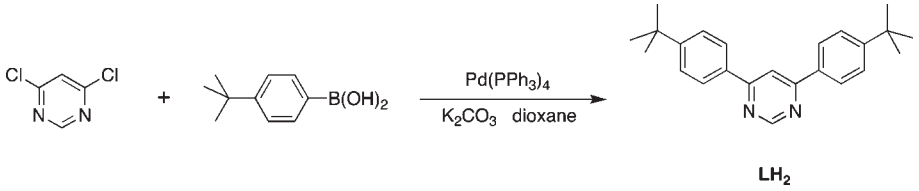

and 3,5-dipyridyl-1,2,4-triazolate were used in two early studies linking $Ir(ppy)_2$ and $Ru(bpy)_2$ units,[15,16] but the pyrazine-type bridges introduced severe nonradiative decay.[17] Steel and co-workers described the bis-cyclopalladation of bis-aryl-pyrimidines, -pyrazines, and -pyridazines,[18] and, more recently, Rourke and co-workers prepared a set of homometallic dinuclear Pd(II) and Pt(II) complexes with 3,6-diphenylpyridazines, though excited-state properties were considered in neither case.[19] Ivanova and colleagues observed luminescence at 77 K from charged, homometallic dinuclear Pd(II) and Pt(II) complexes of 4,6-diphenylpyrimidine.[20] Otherwise, such chemistry has not been extended to the design of luminescent Pt(II) or Ir(III) complexes. Indeed, there are apparently no mixed-metal polymetallic, cyclometalated complexes having both Pt(II) and Ir(III) cyclometalated metal centers present in a single integrated luminophore, despite the potentially interesting properties that might be anticipated.

In this contribution, we describe the synthesis of a rigid, polynuclear cyclometalated complex incorporating one Ir(III) and two Pt(II) centers, using doubly metalated 4,6-di-(4-*tert*-butylphenyl)-pyrimidine as a bridging ligand. The corresponding monometallic complexes and a related dinuclear platinum(II) complex have also been prepared. All of these complexes are intensely luminescent, and the trends in excited state energies are interpreted with the aid of computational and electrochemical studies.

RESULTS

1. Synthesis of Complexes. The synthetic strategy used to prepare the target complexes is depicted in Schemes 1 and 2. The key proligand 4,6-di-(4-*tert*-butylphenyl)pyrimidine, $\mathbf{LH_2}$, was synthesized by a Suzuki cross-coupling reaction of 4,6-dichloropyrimidine with 2.6 equiv of 4-*tert*-butylbenzeneboronic acid (Scheme 1). The *tert*-butyl functionality was introduced to increase the solubility of the final metal complexes, and also to inhibit aggregation of the Pt(II) compounds, a phenomenon commonly encountered with square-planar d^8 metal complexes.[21]

The mono- and dinuclear Pt(II) complexes, Pt($N^\wedge C$-LH)(acac) and $[Pt(acac)]_2\{\mu$-($N^\wedge C$-L-$N^\wedge C$)} (which will be henceforth be referred to respectively as **Pt** and $\mathbf{Pt_2}$) were obtained from the dichloro-bridged intermediates by heating a mixture of the proligand with, respectively, 1 or 2 equiv of K_2PtCl_4 in acetic acid (Scheme 2). The highly insoluble precipitates were collected by filtration and treated with hot dimethylsulfoxide followed by sodium acetylacetonate to give complexes **Pt** and $\mathbf{Pt_2}$ in yields of 52 and 30%, respectively. The corresponding mononuclear iridium complex Ir($N^\wedge C$-LH)$_2$(acac) (referred to as **Ir**) was prepared from $\mathbf{LH_2}$ upon reaction with $IrCl_3 \cdot 3H_2O$ (2.2: 1 molar ratio), followed by treatment with excess sodium acetylacetonate, without isolation of the intermediate dichloro-bridged dimer. An analogous reaction of $IrCl_3 \cdot 3H_2O$ with the complex **Pt** in place of $\mathbf{LH_2}$ as the N$^\wedge$C ligand led to the trinuclear, heterometallic complex Ir$\{\mu$-($N^\wedge C$-L-$N^\wedge C$)Pt(acac)$\}_2$(acac) ($\mathbf{Pt_2Ir}$) in 42% yield. All four complexes were very soluble in dichloromethane owing to the *tert*-butyl groups, and their purification was easily accomplished by using standard column chromatography. The products were characterized by NMR spectroscopy, mass spectrometry, and elemental analysis. Proton NMR spectra are well-resolved and straightforward to interpret because of the presence of a number of characteristic signals. Even in the most complex structure of $\mathbf{Pt_2Ir}$, all 15 signals in the spectrum can be assigned to the structure (see Supporting Information − Section 2).

2. Electrochemistry. The ground-state oxidation and reduction processes exhibited by the four complexes were probed using cyclic voltammetry in dichloromethane solution over the range −2.5 to 1.5 V (potentials versus the ferrocene/ferrocenium couple). Data are listed in Table 1. The mononuclear platinum complex **Pt** displays one quasi-reversible oxidation process within the potential window investigated, at 0.17 V versus Fc|Fc$^+$ (Supporting Information − Section 3). This behavior contrasts with that typically observed for analogous complexes with simple arylpyridine ligands, where the oxidation processes are generally chemically irreversible and appear at more positive potentials; for example, for Pt($N^\wedge C$-ppy)(dpm), $E_p^{ox} = +1.0$ V in DMF versus Fc|Fc$^+$.[22] The irreversibility in such cases is generally attributed to the susceptibility of the electrogenerated Pt(III) species to nucleophilic attack by the solvent. Thus, the chemical reversibility in the present instance, as well as the substantially lower potential of the oxidation, suggests that the resulting charge may be more delocalized over the pyridimine-based cyclometallating ligand than in the pyridyl analogues. Meanwhile, the complex **Pt** undergoes one quasi-reversible reduction process at −2.17 V. The potential of this process is of a similar magnitude to that displayed by a number of Pt(N$^\wedge$C)(O$^\wedge$O) complexes, wherein reduction is assumed to be largely ligand-localized.[22]

The dinuclear complex $\mathbf{Pt_2}$ displays two quasi-reversible oxidation processes at 0.27 and 0.56 V (Figure 1). These may reasonably be attributed to oxidation associated with each of the two metalated units of the ligand, the oxidation of the monocation being expected to be somewhat disfavored compared to the charge-neutral complex. On the other hand, only one reduction process is observed. This would be consistent with the reduction being based on the single heterocyclic ring of the ligand, as in complexes of other aryl-heterocycle ligands such as phenylpyridine, where reduction is thought to occur primarily at the pyridyl ring. The anodic shift of this reduction process compared to **Pt** (the potentials are −1.93 and −2.16 V for $\mathbf{Pt_2}$ and **Pt** respectively) indicates that the introduction of the second platinum(II) center stabilizes the system with respect to reduction.

The mononuclear iridium(III) complex **Ir** displays one reversible oxidation at 0.00 V (the same potential as Fc|Fc$^+$) (Supporting Information − Section 3), but no reduction wave

dx.doi.org/10.1021/ic200706e |*Inorg. Chem.* 2011, 50, 6304–6313

Scheme 2. Preparation of the Mononuclear Complexes (Ir and Pt), the Homometallic Dinuclear Compound (Pt_2), and the Trinuclear Complex (Pt_2Ir), from Proligand LH_2

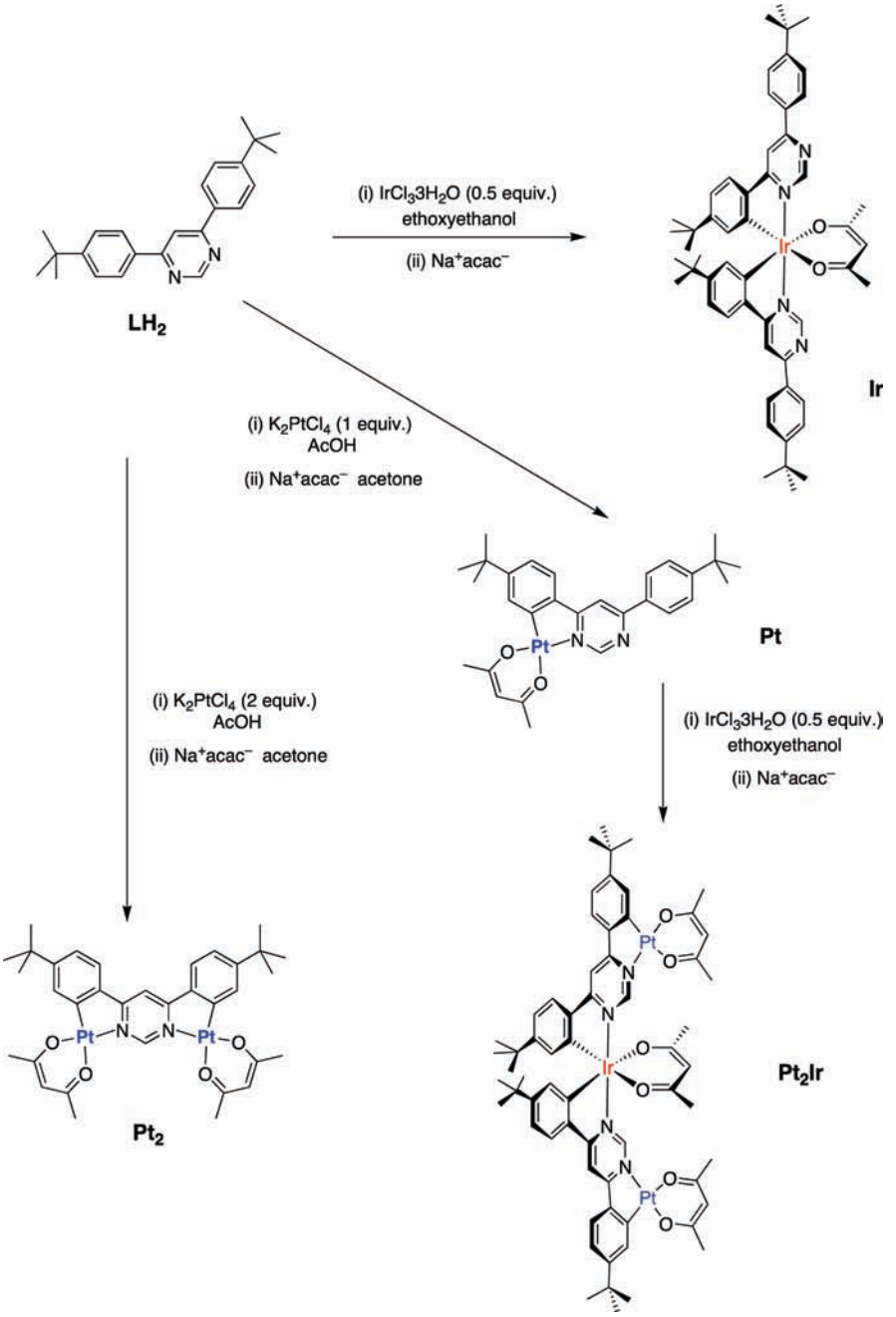

is observed within the accessible solvent window. This pattern of behavior is consistent with that normally exhibited by $Ir(N^{\wedge}C)_2(acac)$ complexes.[23] As in the case of platinum, the oxidation process is seen to be facilitated compared to complexes of arylpyridines; for example, for $Ir(ppy)_2(acac)$, $E_{1/2}^{ox}$ = 0.45 V versus $Fc|Fc^+$. Again, this implies that the pyrimidine unit is able to stabilize the resulting cationic species.

In the trinuclear, mixed-metal complex **Pt_2Ir**, three close-lying oxidation processes can be discerned (Figure 2), though they are not clearly resolved by cyclic voltammetry. Square-wave voltammetry allows them to be discriminated more readily. These processes can reasonably be attributed to oxidations associated with each of the three arylated metals and, based on the values for the mononuclear complexes, it seems likely that the Ir center would undergo oxidation first. It is noticeable, however, that even the first oxidation process for this compound is substantially shifted anodically compared to that of **Ir**, indicating that the presence of the two platinum(II) cations makes the system less readily oxidized. Two reversible reduction waves are observed, at potentials similar to those found for **Pt** and **Pt_2**, an observation again supportive of the notion that reduction is based on the pyrimidine rings.

3. Absorption Spectroscopy. The UV−visible absorption spectra of the four complexes in dichloromethane solution at

dx.doi.org/10.1021/ic200706e |*Inorg. Chem.* 2011, 50, 6304–6313

Table 1. Ground-State Oxidation and Reduction Potentials and UV-visible Absorption Data for the Four Complexes and Proligand LH_2.[a]

complex	absorption λ_{max} / nm (ε/M^{-1} cm^{-1})	$E_{1/2}^{ox}$ / V (ΔE/mV)[b]	$E_{1/2}^{red}$ / V (ΔE/mV)[b]
proligand $\mathbf{LH_2}$	304 (24500), 289 (24200), 259 (25000)		
Pt	399 (11900), 338sh (18500), 308 (38100), 255 (26000)	0.17 (200)	−2.16 (240)
$\mathbf{Pt_2}$	530 (1430), 474 (24500), 417 (16600), 396 (12200), 333 (47200), 256 (36900)	0.14 (160)	−1.93 (180)
		0.43 (220)	
Ir	513 (6210), 497sh (6050), 421 (12600), 376 (20200), 308 (63500), 278 (50800)	0.00 (180)	[c]
$\mathbf{Pt_2Ir}$	568 (13100), 536 (11400), 470 (26300), 443 (24400), 410 (24800), 388 (24500),	0.44 [d]	−2.10 (120)
	330 (69700), 278 (41900), 256 (51300)	0.77[d]	−2.33 (140)
		1.02[d]	

[a] In CH_2Cl_2 at 298 ± 3 K. [b] Potentials obtained by cyclic voltammetry, using Bu_4NPF_6 (0.1 M) as the supporting electrolyte. Potentials are given relative to the $Fc|Fc^+$ couple measured under the same conditions. [c] No reduction wave was observed for this complex within the accessible solvent window. [d] The three oxidations observed for this complex are overlapping in the CV. The quoted values are therefore those obtained by square-wave potentiometry.

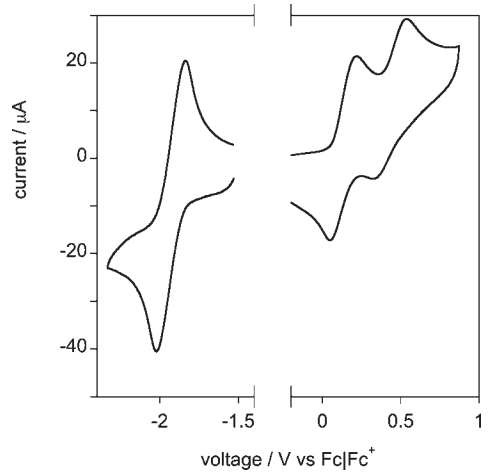

Figure 1. Cyclic voltammograms showing the first reduction and first two oxidation processes of $\mathbf{Pt_2}$ in CH_2Cl_2 at room temperature.

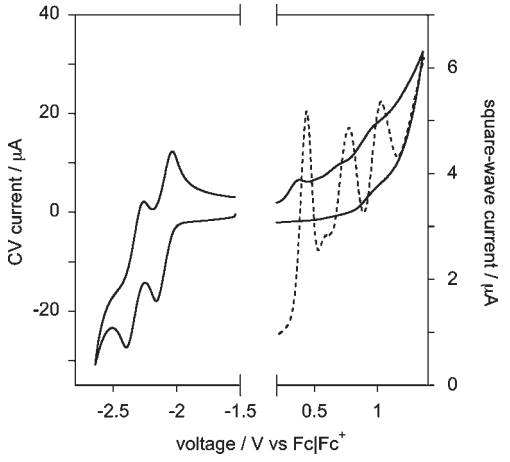

Figure 2. Cyclic voltammograms showing the first two reductions and the first three oxidation processes of $\mathbf{Pt_2Ir}$ in CH_2Cl_2 at room temperature (solid line). The oxidation processes are more clearly resolved using square-wave voltammetry (dashed line).

ambient temperature, together with the spectrum of proligand $\mathbf{LH_2}$ under the same conditions, are shown in Figure 3. The main absorbance maxima and their extinction coefficients are compiled in Table 1. The mononuclear platinum complex **Pt** displays intense bands in the far-UV region around 250−260 nm, similar to those observed for the proligand, and attributed to ligand-based $\pi-\pi^*$ transitions. As typically observed for cyclometalated Pt complexes,[24] including those such as Pt(ppy)(acac),[22] there is an additional set of bands extending into the visible region beyond 400 nm. On the basis of many previous studies,[22,24] and on time-dependent density functional theory (TD-DFT) studies in the present case (vide infra), at least some of these bands can be attributed to charge-transfer transitions from the aryl−metal unit to the heterocyclic ring. The mononuclear iridium complex **Ir** displays a set of bands that extend further into the visible region, beyond 500 nm. This contrasting behavior of iridium(III) compared to platinum(II) with a given cyclometallating ligand mirrors the trend observed for complexes with N^C-coordinating aryl-pyridine ligands, where bis-cyclometalated Ir complexes invariably absorb out to longer wavelengths than their monocyclometalated Pt counterparts.[25] It may be tempting to interpret this in part to the more facile oxidation of the iridium(III) systems, as in the current instance (E^{ox} = 0.00 compared to 0.17 V for the mononuclear Ir and Pt complexes respectively), although such a simplistic argument overlooks the fact that the ligand-based reduction in the Ir complexes is frequently cathodically shifted to such an extent that it lies beyond the normally accessible solvent window. Moreover, transitions involving direct absorption to triplet states may also contribute to the low-energy region of the spectrum, and the spin−orbit coupling pathways that facilitate such processes are typically more efficient for octahedral complexes of d^6 metal ions than for square planar complexes of d^8 metal ions with comparable spin-orbit coupling constants,[5b,26] leading to more significant triplet contributions to the absorption spectrum of iridium complexes.

The spectrum of the dinuclear platinum complex $\mathbf{Pt_2}$ is quite different from its mononuclear counterpart. It displays a very strong absorption band ($\varepsilon \sim 25000$ $M^{-1}cm^{-1}$) at substantially longer wavelength (474 nm) than the longest wavelength band of **Pt**. There is also an additional, weaker low-energy band apparent at 530 nm, which may tentatively be attributed to direct excitation to the triplet state (vide infra). Clearly, the dinuclear system

dx.doi.org/10.1021/ic200706e |*Inorg. Chem.* 2011, 50, 6304–6313

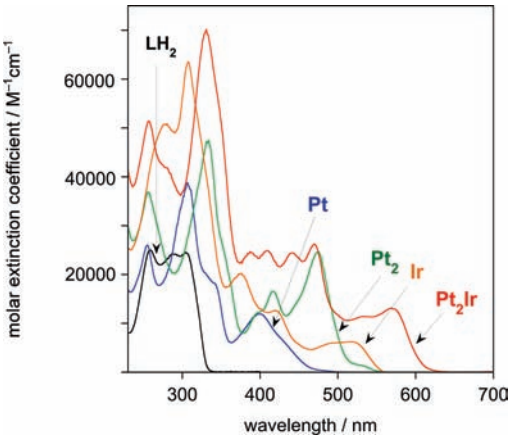

Figure 3. UV−visible absorption spectra of the metal complexes in CH_2Cl_2 solution at 298 K, together with the spectrum of the proligand $\mathbf{LH_2}$ under the same conditions. Legend: **Pt** = blue line; $\mathbf{Pt_2}$ = green; **Ir** = orange; $\mathbf{Pt_2Ir}$ = red; LH_2 = black.

does not behave simply as two interconnected, discrete mononuclear platinum units, since in that case, the band positions would be expected to be similar to those in **Pt**, albeit with higher ε values. The introduction of the second platinum ion has a more profound effect on the excited state properties.

The mixed-metal trinuclear complex $\mathbf{Pt_2Ir}$ is striking in that it is vivid red in color, in contrast to the yellow or orange colors of the other complexes. Its absorption spectrum reveals strong bands that extend out to 600 nm, substantially lower in energy than those displayed by either of the constituent mononuclear units **Pt** and **Ir**. A series of bands in the 370−500 nm region are around twice as intense as those of **Ir** in the same region.

4. Photoluminescence Properties. All four complexes are highly luminescent, both in the solid state and in solution at room temperature. Key photoluminescence parameters are summarized in Table 2. The emission spectra at ambient temperature in solution and at 77 K are shown in Figure 4, together with the spectrum of $\mathbf{LH_2}$ at 77 K for comparison. There is no detectable emission from the proligand at room temperature, but at 77 K phosphorescence is observed. From the position of its 0,0 band, the energy of the triplet state in the proligand is estimated to be 23500 cm^{-1}. The introduction of the metal ions is seen to induce a stabilization of the triplet state, as always observed upon cyclometalation. The trend in emission λ_{max}, **Pt** < $\mathbf{Pt_2}$ < **Ir** < $\mathbf{Pt_2Ir}$, mirrors that observed for the lowest-energy absorption bands. In particular, the dinuclear platinum complex $\mathbf{Pt_2}$ shows no detectable emission bands corresponding to the mononuclear unit. Likewise, the mixed-metal trimer $\mathbf{Pt_2Ir}$ shows no emission bands corresponding to the **Pt** unit. Excitation spectra match closely the absorption spectra. As in absorption, the multinuclear systems are thus again seen to behave as phosphors that are intrinsically different from their constituent units.

At room temperature, vibrational structure is just discernible in the mononuclear platinum complex, while it is more clear-cut in the dinuclear compound. At 77 K (Figure 4b), the structure becomes well-resolved in both cases, showing a vibrational

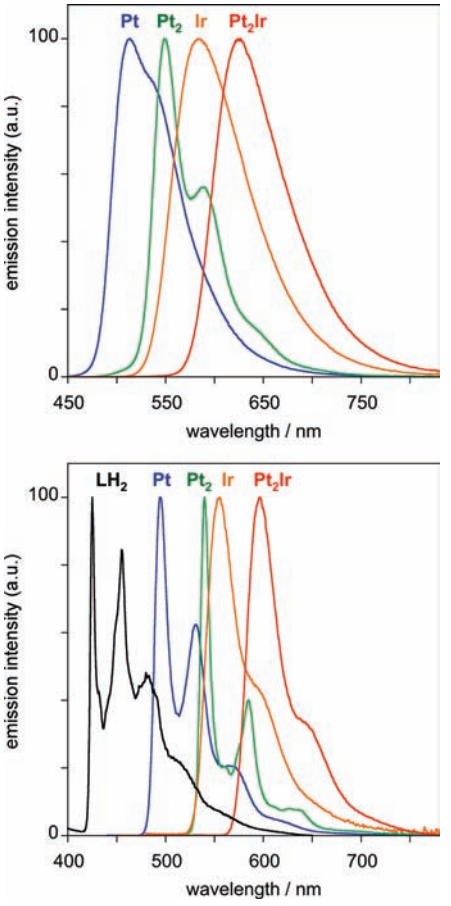

Figure 4. (a) Top: Emission spectra of the four metal complexes in CH_2Cl_2 solution at 298 K. (b) Bottom: Emission spectra of the complexes and of proligand $\mathbf{LH_2}$ at 77 K in diethyl ether/isopentane/ethanol (2:2:1 v/v). Color scheme as in Figure 3.

Table 2. Luminescence Data for the Metal Complexes at 298 K in CH_2Cl_2 and at 77 K (Including Proligand LH_2) in EPA[a]

							emission 77 K	
compound	emission λ_{max}/nm	Φ_{lum}	τ/ns[b]	$k^{Q}_{O2}/10^8$ M^{-1} s^{-1}[c]	$k_r/10^5$ s^{-1}[d]	$\Sigma k_{nr}/10^5$ s^{-1}[d]	λ_{max}/nm	τ/μs
Pt	513, 536sh	0.31	2100 (340)	11	1.5	3.3	494, 531, 569, 616	5.6
$\mathbf{Pt_2}$	550, 591, 647	0.54	1700 (650)	4.3	3.2	2.7	540, 561, 575sh, 585, 631	5.8
Ir	585	0.39	1000 (190)	19	3.9	6.1	554, 595	16
$\mathbf{Pt_2Ir}$	626	0.41	580 (230)	12	7.1	10	596, 643	12
$\mathbf{LH_2}$ proligand	[e]						425, 455, 482, 516	1.8×10^6

[a] EPA = diethyl ether/isopentane/ethanol (2:2:1 v/v). [b] Luminescence lifetime in degassed solution; corresponding values in air-equilibrated solution are given in parentheses. [c] Bimolecular rate constants for quenching by dissolved molecular oxygen, assuming $[O_2] = 2.2$ mmol dm^{-3} in CH_2Cl_2 at 1 atm pressure of air. [d] Radiative (k_r) and nonradiative (Σk_{nr}) decay constants estimated from the measured quantum yields and lifetimes, assuming that the emissive state is formed with unitary efficiency upon excitation. [e] No emission detectable at room temperature.

dx.doi.org/10.1021/ic200706e |*Inorg. Chem.* 2011, 50, 6304–6313

progression of ~1400 cm^{-1} similar to that of the proligand HL_2. The 0,0 component band displays the highest intensity in both cases, indicative of a rigid structure with little distortion upon formation of the excited state compared to the ground state. The spectra of the iridium-containing complexes **Ir** and **Pt_2Ir** are unstructured at room temperature, with a shoulder to the low-energy side visible at 77 K. Such behavior is quite typical of metal complexes with a high degree of metal-to-ligand charge-transfer (MLCT) character {for example, the archetypal cases of $[Ru(bpy)_3]^{2+}$ and $Ir(ppy)_3$},[27] while more structured spectra are generally associated with an increased contribution of ligand-centered character to the excited state.

The quantum yields are high in each case (0.31−0.54, Table 2). It is particularly noticeable that a high value is retained even for the lowest-energy, red-emitting complex **Pt_2Ir**, whereas the efficiency of many metal-based phosphors tends to fall off toward the red, owing to increased nonradiative decay processes through coupling to low-energy vibrations.[28,29] The luminescence lifetimes are of the order of a microsecond, a little less for **Pt_2Ir**, and a little more for the platinum complexes. Assuming that the emitting state is formed with unitary efficiency upon photoexcitation, the radiative (k_r) and nonradiative (Σk_{nr}) decay constants can be estimated from the measured lifetimes and quantum yields (Table 2). Two trends emerge from a consideration of the k_r values. First, the values for the iridium-containing complexes are larger than for the platinum-only complexes. This is quite typical for iridium(III) versus platinum(II) complexes of the same ligands,[25] and is a further reflection of the more efficient spin−orbit coupling pathways associated with an octahedral metal center compared to a square-planar one with similar ζ. The presence of three degenerate filled d orbitals in the former case facilitates the mixing of the triplet state with higher-lying ^{1}MLCT states.[26]

Second, comparing **Pt_2** with **Pt**, it can be seen that k_r increases upon introduction of the second metal center, despite the emission energy decreasing. Other things being equal, a *decrease* in the radiative rate would be expected as the energy decreases, according to the Einstein coefficient which depends on ν^3. Likewise, the presence of the platinum centers in **Pt_2Ir** is seen to enhance k_r compared to that of **Ir**, despite the emission energy of the former being lower. The k_r value roughly doubles on going from **Pt** to **Pt_2** and likewise from **Ir** to **Pt_2Ir**. Apparently, therefore, the $T_1 \rightarrow S_0$ process is promoted by the presence of the additional metal center(s). It might be intuitively reasonable to attribute this effect to the spin−orbit coupling of the extra metal ions facilitating intersystem crossing. However, it can be seen from the absorption spectra (Figure 3) that the $S_0 \rightarrow S_1$ process also increases in intensity from **Pt** to **Pt_2** and from **Ir** to **Pt_2Ir** (by a similar 2-fold factor to the increase in triplet k_r in each case), suggesting that the oscillator strength also increases for the spin-allowed singlet transitions. These conclusions are supported by the results of calculations discussed in the next section.

5. TD-DFT Calculations. To facilitate the interpretation of the electrochemical and photophysical results, TD-DFT calculations have been carried out on the molecules, both in the gas phase and in dichloromethane solution using the polarized continuum solvent model.[30] We have also included the hypothetical complex Pt(acac){μ-($N^\wedge C$-L-$N^\wedge C$)}Ir(acac)($N^\wedge C$-LH) (**PtIr**) for comparison. The B3LYP functional was used, with the LanL2DZ basis set for Pt and Ir and 6-31+G(d) basis set for all other atoms, as implemented in Gaussian09W.[31] Full geometry optimizations were carried out, but the larger complexes **Ir**, **PtIr**, and **Pt_2Ir** were truncated by removal of the *tert*-butyl groups to keep the job times manageable. The optimized geometry of proligand **LH_2** shows twists of 14° and 16° in the dihedral angle between the central pyrimidine and the noncoordinated flanking aryl rings, reflecting the anticipated opposing balance between conjugation and steric effects. In the complexes, the dihedral angles for the equivalent noncoordinated aryl rings range from 6° (**Ir**) to 16° (**PtIr**), while the coordinated aryl rings are essentially coplanar with the pyrimidine ring in each case (dihedral angles <1.5°). The calculated Pt−C and Pt−N bond lengths for the four Pt moieties range from 1.980 to 1.983 Å and from 2.020 to 2.036 Å, respectively, while the Ir−C and Ir−N bond lengths for the three Ir units are in the range 2.001−2005 Å and 2.053−2.065 Å respectively. Each Pt center has one longer and one shorter Pt−O bond, in the ranges of 2.147−2.153 Å and 2.036−2.044 Å, respectively, reflecting the subtly greater C═O double bond character trans to the metalated carbon (higher trans influence than N) and, conversely, C−O^- trans to the pyrimidine N atom. This is also reflected in slightly different C−O and C−C distances in each acac ligand coordinated to Pt. In contrast, the acac ligands on Ir, all of which are trans to carbon, show equivalent C−O and C−C bond lengths; and the Ir−O distances, which span the range of 2.058−2.196 Å, are equivalent in each of the three Ir complexes. All of the calculated bond lengths around Pt and Ir are comparable to those for related complexes of arylpyridines determined by X-ray diffraction.[22,32,24h]

The calculations reveal that the lowest-energy singlet transitions ($S_0 \rightarrow S_1$) are composed predominantly of HOMO→LUMO excitations in each case (Tables S1 and S2 in Supporting Information − Section 4). The frontier orbitals of the Pt complexes are shown in Figure 5. In the mononuclear **Pt** complex, the highest occupied molecular orbital (HOMO) is seen to be based primarily on the metalated aryl ring and the metal, whereas the LUMO is mostly localized on the pyrimidine ring. Such a trend has been commonly encountered in complexes of arylpyridines, and is consistent with the usual $d_{Pt}/\pi_{N^\wedge \underline{C}} \rightarrow \pi^*_{\underline{N}^\wedge C}$ assignment of the emissive excited state.[24] In the dinuclear complex **Pt_2**, the pattern for the HOMO is similar, being based on each metalated aryl ring, with little conjugation apparent between the two halves of the molecule. In contrast, the LUMO is delocalized over both units and the central pyrimidine. We can thus expect a stabilization of the LUMO upon introduction of the second platinum center, with little effect on the HOMO, and indeed the calculated energies of the orbitals reveal this to be the case; the HOMO energies for **Pt** and **Pt_2** in vacuo are −5.72 and −5.73 eV, respectively, while the LUMO energies are −2.28 and −2.51 eV, respectively.

This conclusion is consistent with the electrochemical results, where the reduction potential was anodically shifted in **Pt_2** compared to **Pt**, while there was little effect on the oxidation potential. As a result of the stabilization of the LUMO, the HOMO→LUMO gap is decreased from 3.52 eV for **Pt** to 3.24 eV for **Pt_2** (calculated values in CH_2Cl_2; the corresponding value calculated for the proligand is 4.49 eV). This trend is in line with the observed shift of the lowest energy absorption band to longer wavelengths on going from **LH_2** to **Pt** to **Pt_2**. The absorption spectra simulated on the basis of the TD-DFT results are shown in Figure 6 and, indeed, they reveal a good match to the observed spectra of Figure 3, in terms not only of the positions of the bands, but also their relative intensities. In addition, a calculation including the triplet excited states for **Pt_2** in dichloromethane placed the formally spin-forbidden $S_0 \rightarrow T_1$ transition at 537 nm (predominantly HOMO→LUMO), in good agreement with the observed weak band at 530 nm.

dx.doi.org/10.1021/ic200706e |*Inorg. Chem.* 2011, 50, 6304–6313

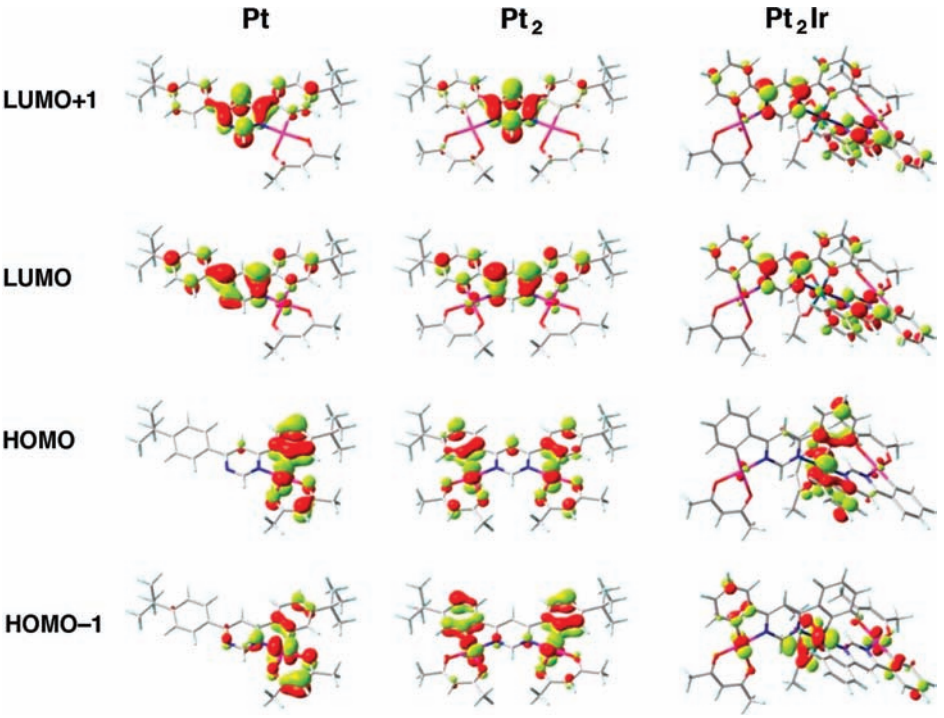

Figure 5. Frontier orbitals of the mononuclear and dinuclear platinum complexes and of the mixed-metal trinuclear complex, obtained by TD-DFT, plotted at an isovalue of 0.04.

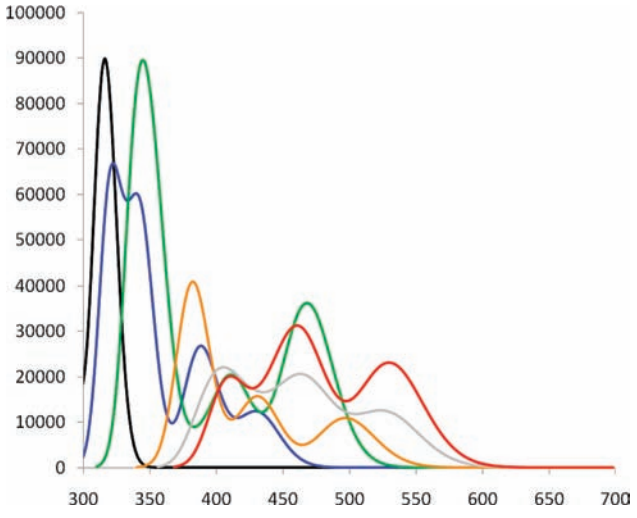

Figure 6. Simulated UV−visible absorption spectra of the compounds by TD-DFT calculations with CH_2Cl_2 implicit solvent model. Colors as in Figure 3, namely, black, **LH_2**; blue, **Pt**; green, **Pt_2**; orange, **Ir**; red, **Pt_2Ir**; in addition, the spectrum of the hypothetical complex **PtIr** is included in gray.

The calculated spectrum of the hypothetical complex **PtIr** is very similar to that of **Pt_2Ir**, and the HOMO→LUMO gaps for these two complexes are identical (2.99 eV in dichloromethane, compared to 3.18 eV for **Ir**), confirming that the key determinant of the energy of the lowest-energy band is the presence of the two different metals.[33] It may also be noted that the calculations reveal a significant increase in the oscillator strength of the lowest-energy transitions on going from **Pt** to **Pt_2** and from **Ir** to **Pt_2Ir** (Supporting Information, Tables S1 and S2 and Figure 6). This is consistent with the experimental results of absorption spectroscopy discussed in Section 4, a trend that was also apparent in the radiative rate constants of emission from the corresponding triplet states.

CONCLUDING DISCUSSION

In this work, we have prepared a binuclear platinum complex and a trinuclear heterometallic complex incorporating iridium(III) and platinum(II) ions, in which the metals are cyclometalated to a common ligand leading to an integrated luminophore. The corresponding mononuclear complexes have also been prepared, allowing the influence of the extra metal ions to be probed. The combination of electrochemistry, TD-DFT, absorption and emission spectroscopy reveals that the multimetallic systems behave as chromophores that are intrinsically different from their mononuclear counterparts, owing primarily to the conjugation of the LUMO across the entire aromatic ligand, with the pyrimidine acting as a bridge of communication. Thus, unlike many other multimetallic systems in supramolecular photochemistry, the metallic units do not retain their separate identities, and it is not appropriate to consider them as individual units between which energy transfer occurs. Rather, the introduction of additional metal centers is seen to allow additional control over the excited state properties of the important class of phosphorescent compounds based on cyclometalated metal complexes. In particular, in the present instance, it can be seen that the absorption and emission of an iridium complex can be signficantly shifted further into the red region through introduction of the platinum ions. The ability to shift absorption to the red is desirable, for example, in the absorbing units of dye-sensitized solar cells. Moreover, the augmentation of the radiative rate constants in response to the added metal ions, as well as the rigidity of the systems which keeps nonradiative decay to a minimum, ensures

dx.doi.org/10.1021/ic200706e |*Inorg. Chem.* 2011, 50, 6304–6313

that high emission quantum yields are retained in the red region, a desirable property in, for example, solar concentrators and red phosphors for OLEDs alike. We expect that these first examples, which make use of the versatile aryl pyrimidine unit, will lead to new opportunities for controlling excited states for such contemporary applications.

EXPERIMENTAL SECTION

^{1}H and ^{13}C NMR spectra were recorded on Bruker Avance-400 or JEOL Delta-270 spectrometers operating at the frequencies indicated. Chemical shifts (δ) are in ppm, referenced to residual protio-solvent resonances, and coupling constants are in hertz. Mass spectra were recorded at the EPSRC National Mass Spectrometry Service Centre using MALDI ionization on an Applied Biosystems Voyager instrument, using DCTB as the matrix. Elemental analyses were carried out using a Carlo Erba 1108 Elemental Analyzer controlled with CE Eager 200 software, run in accordance with the manufacturer's instructions and weighed using a certified Mettler MX5Microbalance.

4,6-Di-(4-*tert*-butylphenyl)pyrimidine LH_2. A mixture of 4-*tert*-butylphenylboronic acid (2.0 g, 11.2 mmol), 4,6-dichloropyrimidine (643 mg, 4.3 mmol), 2 M aqueous solution of K_2CO_3 (13 mL, 26 mmol), and 1,4-dioxane was deaerated by bubbling argon through the mixture for 10 min. A catalytic amount of $Pd(PPh_3)_4$ was added, and argon was bubbled through the mixture for an additional 10 min. The reaction mixture was then stirred at 95 °C for 24 h. After completion of the reaction, toluene (20 mL) was added, and the mixture was washed with water. The organic layer was dried over $MgSO_4$ and evaporated to dryness. The product was then purified by column chromatography (silica gel, ethyl acetate/hexane, 1/4) followed by recrystallization from methanol, giving the product as a colorless solid (990 mg, 67%). ^{1}H (270 MHz, $CDCl_3$): δ = 9.27 (d, 1H, J = 1.2), 8.07 (AA′XX′, 4H, J = 8.7), 8.06 (br s, 1H), 7.54 (AA′XX′, 4H, J = 8.7), 1.41 (s, 18H). ^{13}C (68 MHz, $CDCl_3$): δ = 164.5, 159.1, 154.4, 134.3, 127.0, 126.0, 112.3, 34.9, 31.2. Elemental analysis calcd for $C_{24}H_{28}N_2$: C 83.68, H 8.19, N 8.13%; found C 83.75, H 8.06, N 8.12%.

Mononuclear Platinum Complex Pt. A mixture of **LH_2** (450 mg, 1.3 mmol) and potassium tetrachloroplatinate (542 mg, 1.3 mmol) in acetic acid (125 mL) was heated under reflux for 14 h. The solvent was removed by rotary evaporation, and the residue was dissolved in dimethylsulfoxide (DMSO, 20 mL), heated under reflux for 1 min, and allowed to cool to room temperature. Water (70 mL) was added, and the solid that precipitated was filtered off, washed with water, and dissolved in acetone (70 mL). Sodium acetylacetonate (1.6 g, 13 mmol) was added, and the mixture was heated under reflux for 5 h. Water (70 mL) was added, and the precipitated solid was filtered off, washed with water, and dried. Purification by column chromatography (silica gel, CH_2Cl_2) led to the product as a yellow solid (429 mg, 52%). ^{1}H (400 Hz, $CDCl_3$) δ = 9.59 (d, 1H, J = 1.2), 8.12 (AA′XX′, 2H, J = 8.7), 7.84 (d, 1H, J = 1.2), 7.73 (d, 1H, J = 2.0), 7.58 (AA′XX′, 2H, J = 8.7), 7.57 (d, 1H, J = 2.0), 7.23 (dd, 1H, J = 8.2, 2.0), 5.52 (s, 1H), 2.06 (s, 3H), 2.04 (s, 3H), 1.41 (s, 9H), 1.40 (s, 9H). Elemental analysis calcd for $C_{29}H_{34}N_2O_2Pt$: C 54.62, H 5.37, N 4.39%; found C 54.63, H 5.52, N 4.47%. MS (MALDI, DCTB/DCM): m/z = 636.1 $[M]^+$.

Dinuclear Platinum Complex Pt_2. A mixture of **LH_2** (345 mg, 1 mmol) and potassium tetrachloroplatinate (830 mg, 2 mmol) in acetic acid (125 mL) was heated under reflux for 3 days. The solvent was removed by rotary evaporation, the residue dissolved in DMSO (20 mL), heated to reflux for 3 min, and then the solvent was evaporated under reduced pressure. The residue was treated with methanol to give a solid which was filtered off and washed with methanol (470 mg, 58%). A mixture of the above solid (150 mg, 0.19 mmol), sodium acetylacetonate (230 mg, 1.9 mmol), and acetone (75 mL) was heated under reflux for 1 h. Water (75 mL) was added, and the precipitated solid was filtered off, washed with water and acetone (5 mL). The product was then purified by filtering through a short plug of silica gel, which was eluted with a mixture of CH_2Cl_2 and ethyl acetate (10/1). The solvent was evaporated to dryness; the residue was treated with acetone and filtered, to give the product as bright orange crystals (90 mg, 51%). ^{1}H (400 Hz, $CDCl_3$) δ = 9.87 (br s, 1H), 7.63 (d, 2H, J = 2.0), 7.44 (br s, 1H), 7.41 (d, 2H, J = 8.2), 7.14 (dd, 2H, J = 8.2, 2.0), 5.44 (s, 2H), 2.01 (s, 6H), 1.97 (s, 6H), 1.36 (s, 18H). Elemental analysis calcd for $C_{34}H_{40}N_2O_4Pt_2$: C 43.87, H 4.33, N 3.01%; found C 44.00, H 4.25, N 3.20%. MS (MALDI, DCTB/DCM): m/z = 928.2 $[M]^+$.

Mononuclear Iridium Complex Ir. A mixture of **LH_2** (205 mg, 0.6 mmol), $IrCl_3 \cdot 3H_2O$ (95 mg, 0.27 mmol) and ethoxyethanol was heated at 110 °C for 14 h. Sodium acetylacetonate (165 mg, 1.35 mmol) was added, and the mixture was stirred at 90 °C for 5 h. The solvent was removed by rotary evaporation, and the residue purified by column chromatography (silica gel, CH_2Cl_2) to give the product as an orange solid (374 mg, 64%). ^{1}H (400 Hz, $CDCl_3$) δ = 9.17 (d, 1H, J = 1.2), 8.20 (AA′XX′, 4H, J = 8.6), 8.11 (d, 2H, J = 1.2), 7.67 (d, 2H, J = 8.2), 7.63 (AA′XX′, 4H, J = 8.6), 6.95 (dd, 2H, J = 8.2, 1.9), 6.46 (d, 2H, J = 1.9), 5.24 (s, 1H), 1.83 (s, 6H), 1,43 (s, 18H), 1.08 (s, 18H). Elemental analysis calcd for $C_{53}H_{61}IrN_4O_2$: C 65.07, H 6.28, N 5.73%; found C 64.87, H 6.77, N 5.81%. MS (MALDI, DCTB/DCM): m/z = 976.4 $[M]^+$.

Mixed-Metal Trinuclear Complex Pt_2Ir. A mixture of **Pt** (340 mg, 0.53 mmol), $IrCl_3 \cdot 3H_2O$ (85 mg, 0.24 mmol) and ethoxyethanol was heated at 110 °C for 12 h. Sodium acetylacetonate (150 mg, 1.23 mmol) was added, and the mixture was stirred at 80 °C for 4 h. The solvent was removed by rotary evaporation, and the residue was purified by column chromatography (silica gel, CH_2Cl_2, followed by a second column on silica gel, CH_2Cl_2/hexane, 1/1). Fractions with the product were combined and evaporated to dryness. The residue was treated with methanol and filtered to give the product as bright red solid (163 mg, 42%). ^{1}H (270 Hz, $CDCl_3$) δ = 9.35 (d, 2H, J = 0.9), 7.76 (br.s, 2H), 7.68 (d, 2H, J = 1.9), 7.57 (d, 2H, J = 8.5), 7.54 (d, 2H, J = 8.5), 7.19 (dd, 2H, J = 8.2, 2.0), 6.89 (dd, 2H, J = 8.3, 1.9), 6.48 (d, 2H, J = 1.9), 5.40 (s, 2H), 5.20 (s, 1H), 1.96 (s, 6H), 1.84 (s, 6H), 1.80 (s, 6H), 1.34 (s, 18H), 1.01 (s, 18H). Elemental analysis calcd for $C_{63}H_{73}IrN_4O_6Pt_2$: C 48.36, H 4.70, N 3.58%; found C 48.41, H 4.98, N 3.69%. MS (MALDI, DCTB/DCM): m/z = 1560.4 $[M]^+$.

Density Functional Theory Calculations. All DFT calculations were carried out using Gaussian 09W.[31] The B3LYP hybrid functional was used, together with the LanL2DZ basis set for Pt and Ir, and 6-31+G(d) for all other atom types. Geometries were fully optimized in vacuo. UV−vis spectra were obtained by single point TD-DFT calculations at the optimized geometries, using the same functional and basis sets, either in vacuo or with a PCM solvent correction[30] for dichloromethane. The molecular orbitals and spectra were visualized using GaussView 5.0,[34] with Gaussian line shapes and an arbitrary half-width at half-height of 1000 cm^{-1} for the latter.

Electrochemistry. Cyclic voltammetry was carried out using a μAutolab Type III potentiostat with computer control and data storage via GPES Manager software. Solutions of concentration 1 mM in CH_2Cl_2 at 298 ± 3 K were used, containing $[Bu_4N][PF_6]$ as the supporting electrolyte. A three-electrode assembly was employed, consisting of a glassy carbon working electrode, and platinum wire counter and reference electrodes. Solutions were purged for at least 5 min with solvent-saturated nitrogen gas with stirring, prior to measurements being taken under a nitrogen atmosphere without stirring. The voltammograms were referenced to the ferrocence-ferrocenium couple measured under the same conditions.

Photophysical Measurements. Absorption spectra were measured on a Biotek Instruments XS spectrometer, using quartz cuvettes of 1 cm path length. Steady-state luminescence spectra were measured using a Jobin Yvon FluoroMax-2 spectrofluorimeter, fitted with a red-sensitive Hamamatsu R928 photomultiplier tube; the spectra shown are

dx.doi.org/10.1021/ic200706e |*Inorg. Chem.* 2011, 50, 6304–6313

corrected for the wavelength dependence of the detector, and the quoted emission maxima refer to the values after correction. Samples for emission measurements were contained within quartz cuvettes of 1 cm path length modified with appropriate glassware to allow connection to a high-vacuum line. Degassing was achieved via a minimum of three freeze−pump−thaw cycles while connected to the vacuum manifold; final vapor pressure at 77 K was $<5 \times 10^{-2}$ mbar, as monitored using a Pirani gauge. Luminescence quantum yields were determined using $[Ru(bpy)_3]Cl_2$ in degassed aqueous solution as the standard (ϕ = 0.042[35]); estimated uncertainty in Φ is ±20% or better.

The luminescence lifetimes of the complexes were measured by time-correlated single-photon counting, following excitation at 374.0 nm with an EPL-375 pulsed-diode laser. The emitted light was detected at 90° using a Peltier-cooled R928 PMT after passage through a monochromator. The estimated uncertainty in the quoted lifetimes is ±10% or better. Lifetimes at 77 K in excess of 10 μs were measured by multichannel scaling following excitation with a μs-pulsed xenon lamp; an excitation wavelength of 374 nm (band-pass 5 nm) was selected with a monochromator. Bimolecular rate constants for quenching by molecular oxygen, k_Q, were determined from the lifetimes in degassed and air-equilibrated solution, taking the concentration of oxygen in CH_2Cl_2 at 0.21 atm O_2 to be 2.2 mmol dm^{-3}.[36]

■ ASSOCIATED CONTENT

Supporting Information. Original NMR and mass spectra; additional cyclic voltammetry and square-wave potentiometry plots; tabulated data from DFT calculations. This material is available free of charge via the Internet at http://pubs.acs.org.

■ AUTHOR INFORMATION

Corresponding Author

*E-mail: valery.kozhevnikov@northumbria.ac.uk, j.a.g.williams@durham.ac.uk.

■ ACKNOWLEDGMENT

We thank the School of Life Sciences, Northumbria University for funding, the EPSRC National Mass Spectrometry Service Centre, Swansea for recording mass spectra, and Dr V. L. Whittle for assistance with electrochemical measurements.

■ REFERENCES

(1) Chi, Y.; Chou, P.-T. *Chem. Soc. Rev.* **2010**, *39*, 638.

(2) (a) Dixon, I. M.; Collin, J.-P.; Sauvage, J.-P.; Flamigni, L.; Encinas, S.; Barigelletti, F. *Chem. Soc. Rev.* **2000**, *29*, 385. (b) Lowry, M. S.; Bernhard, S. *Chem.—Eur. J.* **2006**, *12*, 7970. (c) Flamigni, L.; Barbieri, A.; Sabatini, C.; Ventura, B.; Barigelletti, F. *Top. Curr. Chem.* **2007**, *281*, 143. (d) Wong, W.-Y.; Ho, C. L. *J. Mater. Chem.* **2009**, *19*, 4457. (e) Williams, J. A. G.; Wilkinson, A. J.; Whittle, V. L. *Dalton Trans.* **2008**, 2081.

(3) (a) Lai, S.-W.; Che, C.-M. *Top. Curr. Chem.* **2004**, *241*, 27. (b) Williams, J. A. G. *Top. Curr. Chem.* **2007**, *281*, 205. (c) Williams, J. A. G.; Develay, S.; Rochester, D. L.; Murphy, L. *Coord. Chem. Rev.* **2008**, *252*, 2596.

(4) (a) Baldo, M. A.; Thompson, M. E.; Forrest, S. R. *Pure Appl. Chem.* **1999**, *71*, 2095.(b) Yersin, H., Ed.; *Highly Efficient OLEDs with Phosphorescent Materials*; Wiley-VCH: Weinheim. Germany, 2008.

(5) (a) Evans, R. C.; Douglas, P.; Winscom, C. J. *Coord. Chem. Rev.* **2006**, *250*, 2093. (b) Rausch, A. F.; Homeier, H. H. H.; Djurovich, P. I.; Thompson, M. E.; Yersin, Y. *Proc. SPIE.* **2007**, *6655*, F6550.(c) Chou, P.-T.; Chi, Y.; Chung, M.-W.; Lin, C.-C. *Coord. Chem. Rev.* **2011**, DOI: 10.1016/J.CCR.2010.12.013

(6) (a) Zhao, Q.; Li, F.; Huang, C. *Chem. Soc. Rev.* **2010**, *39*, 3007. (b) Fletcher, N. C.; Lagunas, M. C. *Top. Organomet. Chem.* **2010**, *28*, 143. (c) Lo, K. K.-W.; Li, S. P.-Y.; Zhang, K. Y. *New J. Chem.* **2011**, *35*, 265.

(7) (a) Yu, M. X.; Zhao, Q.; Shi, L. X.; Li, F. Y.; Zhou, Z. G.; Yang, H.; Yia, T.; Huang, C. *Chem. Commun.* **2008**, 2115. (b) Botchway, S. W.; Charnley, M.; Haycock, J. W.; Parker, A. W.; Rochester, D. L.; Weinstein, J. A.; Williams, J. A. G. *Proc. Natl. Acad. Sci. U.S.A.* **2008**, *105*, 16071. (c) Koo, C. K.; Wong, K. L.; Man, C. W. Y.; Lam, Y. W.; So, K. Y.; Tam, H. L.; Tsao, S. W.; Cheah, K. W.; Lau, K. C.; Yang, Y. Y.; Chen, J. C.; Lam, M. H. W. *Inorg. Chem.* **2009**, *48*, 872. (d) Lo, K.K.-W.; Louie, M. W.; Zhang, K. Y. *Coord. Chem. Rev.* **2010**, *254*, 2603. (e) Fernandez-Moreira, V.; Thorp-Greenwood, F. L.; Coogan, M. P. *Chem. Commun.* **2010**, *56*, 186. (f) Murphy, L.; Congreve, A.; Palsson, L. O.; Williams, J. A. G. *Chem. Commun.* **2010**, *46*, 8743. (g) Zhao, Q.; Huang, C.; Li, F. *Chem. Soc. Rev.* **2011**, *40*, 2508.

(8) (a) Lowry, M. S.; Goldsmith, J. I.; Slinker, J. D.; Rohl, R.; Pascal, R. A., Jr.; Malliaras, G. G.; Bernhard, S. *Chem. Mater.* **2005**, *17*, 5712. (b) Curtin, P.; Tinker, L. L.; Burgess, C. M.; Cline, E. D.; Bernhard, S. *Inorg. Chem.* **2009**, *48*, 10499.

(9) Campagna, S.; Puntoriero, F.; Nastasi, F.; Bergamini, G.; Balzani, V. *Top. Curr. Chem.* **2007**, *280*, 117.

(10) (a) Arm, K. J.; Williams, J. A. G. *Chem. Commun.* **2005**, 230. (b) Sabatini, C.; Barbieri, A.; Barigelletti, F.; Arm, K. J.; Williams, J. A. G. *Photochem. Photobiol. Sci.* **2007**, *6*, 397.

(11) (a) Lai, S.-W.; Chan, M. C.-W.; Cheung, T. C.; Peng, S.-M.; Che, C.-M. *Inorg. Chem.* **1999**, *38*, 4046. (b) Lai, S.-W.; Lam, H.-W.; Lu, W.; Cheung, K.-K.; Che, C. M. *Organometallics* **2002**, *21*, 226. (c) Ma, B.; Li, J.; Djurovich, P. I.; Yousufuddin, M.; Bau, R.; Thompson, M. E. *J. Am. Chem. Soc.* **2005**, *127*, 28. (d) Ma, B.; Djurovich, P. I.; Garon, S.; Alleyne, B.; Thompson, M. E. *Adv. Funct. Mater.* **2006**, *16*, 2438. (e) Develay, S.; Williams, J. A. G. *Dalton Trans.* **2008**, 4562. (f) Tong, W.-L.; Chan, M. C.-W.; Yiu, S.-M. *Organometallics* **2010**, *29*, 6377.

(12) (a) Welter, S.; Lafolet, F.; Cecchetto, E.; Verrgeer, F.; De Cola, L. *ChemPhysChem* **2005**, *6*, 2417. (b) Welter, S.; Salluce, N.; Belser, P.; Groeneveld, M.; De Cola, L. *Coord. Chem. Rev.* **2005**, *249*, 1360. (c) Arm, K. J.; Williams, J. A. G. *Dalton Trans.* **2006**, 2172.

(13) (a) Neve, F.; Crispini, A.; Serroni, S.; Loiseau, F.; Campagna, S. *Inorg. Chem.* **2001**, *40*, 1093. (b) Auffrant, A.; Barbieri, A.; Barigelletti, F.; Colin, J.-P.; Flamigni, L.; Sabatini, C.; Sauvage, J.-P. *Inorg. Chem.* **2006**, *45*, 10990. (c) Whittle, V. L.; Williams, J. A. G. *Inorg. Chem.* **2008**, *47*, 6597. (d) Whittle, V. L.; Williams, J. A. G. *Dalton Trans.* **2009**, 3929.

(14) (a) Ma, B.; Djurovich, P. I.; Yousufuddin, M.; Bau, R.; Thompson, M. E. *J. Phys. Chem.* **2006**, *112*, 8022. (b) Shin, C. H.; Huh, J. O.; Baek, S. J.; Kim, S. K.; Lee, M. H.; Do, Y. *Eur. J. Inorg. Chem.* **2010**, 3642.

(15) Ortmans, I.; Didier, O.; Kirsch-Demesmaeker, A. *Inorg. Chem.* **1995**, *34*, 3695.

(16) Vandiemen, J. H.; Hage, R.; Haasnoot, J. G.; Lempers, H. E. B.; Reedijk, J.; Vos, J. G.; De Cola, L.; Barigelletti, F.; Balzani, V. *Inorg. Chem.* **1992**, *31*, 3518.

(17) Serroni, S.; Juris, A.; Campagna, S.; Venturi, M.; Denti, G.; Balzani, V. *J. Am. Chem. Soc.* **1994**, *116*, 9086.

(18) Caygill, G. B.; Hartshorn, R. M.; Steel, P. J. *J. Organomet. Chem.* **1990**, *395*, 359.

(19) (a) Slater, J. W.; Lydon, D. P.; Alcock, N. W.; Rourke, J. P. *Organometallics* **2001**, *20*, 4418. (b) Slater, J. W.; Rourke, J. P. *J. Organomet. Chem.* **2003**, *688*, 112.

(20) (a) Ivanova, E. V.; Puzyk, M. V.; Balashev, K. P. *Zh. Odshch. Kim* **2008**, *78*, 1008. (b) *Idem, ibid.* **2009**, *79*, 1600. (c) *Idem, Opt. Spectrosc.* **2009**, *106*, 359.

(21) Miller, J. S., Ed.; *Extended linear chain compounds*; Plenum Press: New York, 1982.

(22) Brooks, J.; Babayan, Y.; Lamansky, S.; Djurovich, P. I.; Tsyba, I.; Bau, R.; Thompson, M. E. *Inorg. Chem.* **2002**, *41*, 3055.

(23) (a) Lamansky, S.; Djurovich, P.; Murphy, D.; Abdel-Razzaq, F.; Kwong, R.; Tsyba, I.; Bortz, M.; Mui, B.; Bau, R.; Thomspon, M. E. *Inorg. Chem.* **2001**, *40*, 1704. (b) Lamansky, S.; Djurovich, P.; Murphy, D.;

Abdel-Razzaq, F.; Lee, H. E.; Adachi, C.; Burrows, P. E.; Forrest, S. R.; Thompson, M. E. *J. Am. Chem. Soc.* **2001**, *123*, 4304.

(24) (a) Balashev, K. P.; Puzyk, M. V.; Kotlyar, V. S.; Kulikova, M. V. *Coord. Chem. Rev.* **1997**, *159*, 109. (b) Yin, B. L.; Niemeyer, F.; Williams, J. A. G.; Jiang, J.; Boucekkine, A.; Toupet, L.; Le Bozec, H.; Guerchais, V. *Inorg. Chem.* **2006**, *45*, 8584. (c) Niedermair, F.; Kwon, O.; Zojer, K.; Kappaun, S.; Trimmel, G.; Mereiter, K.; Slugovc, C. *Dalton Trans.* **2008**, 4006. (d) Ghedini, M.; Pugliese, T.; La Deda, M.; Godbert, N.; Aiello, I.; Amati, M.; Belviso, S.; Lelj, F.; Accorsi, G.; Barigelletti, F. *Dalton Trans.* **2008**, 4303. (e) Chang, S.-Y.; Cheng, Y.-M.; Chi, Y.; Lin, Y.-C.; Jiang, C.-M.; Lee, G.-H.; Chou, P.-T. *Dalton Trans.* **2008**, 6901. (f) Develay, S.; Blackburn, O.; Thompson, A. L.; Williams, J. A. G. *Inorg. Chem.* **2008**, *47*, 11129. (g) Wong, W.-Y.; Ho, C.-L. *J. Mater. Chem.* **2009**, *19*, 4457. (h) Santoro, A.; Whitwood, A. C.; Williams, J. A. G.; Kozhevnikov, V. N.; Bruce, D. W. *Chem. Mater.* **2009**, *21*, 3871. (i) Zhou, G.; Wang, Q.; Ho, C.-L.; Wong, W.-Y.; Ma, D.; Wang, L. *Chem. Commun.* **2009**, 3574. (j) Vezzu, D. A. K.; Deaton, J. C.; Jones, J. S.; Bartolotti, L.; Harris, C. F.; Marchetti, A. P.; Kondakova, M.; Pike, R. D.; Huo, S. *Inorg. Chem.* **2010**, *49*, 5107.

(25) Contrast, for example, data in refs 22 and 23 (Pt and Ir, respectively, with arylpyridine ligands). For a recent integral study examining both Pt and Ir complexes having cyclometallated ligands in common (e.g., thienylpyridine and derivatives), see: Kozhevnikov, D. N.; Kozhevnikov, V. N.; Shafikov, M. Z.; Prokhorov, A. M.; Bruce, D. W.; Williams, J. A. G. *Inorg. Chem.* **2011**, *50*, 3804.

(26) Yersin, H.; Rausch, A. F.; Czerwieniec, R.; Hofbeck, T.; Fischer, T. *Coord. Chem. Rev.* **2010**, DOI: 10.1016/j.ccr.2011.01.042

(27) Watts, R. J. *J. Chem. Educ.* **1983**, *60*, 834.

(28) (a) Kober, E. M.; Caspar, J. V.; Lumpkin, R. S.; Meyer, T. J. *J. Phys. Chem.* **1986**, *90*, 3722. (b) Barqawi, K. R.; Murtaza, Z.; Meyer, T. J. *J. Phys. Chem.* **1991**, *95*, 47.

(29) Whittle, C. E.; Weinstein, J. A.; George, M. W.; Schanze, K. S. *Inorg. Chem.* **2001**, *40*, 4053.

(30) Cossi, K.; Scalmani, G.; Rega, N.; Barone, V. *J. Chem. Phys.* **2002**, *117*, 43.

(31) Frisch, M. J.; Trucks, G. W.; Schlegel, H. B.; Scuseria, G. E.; Robb, M. A.; Cheeseman, J. R.; Scalmani, G.; Barone, V.; Mennucci, B.; Petersson, G. A.; Nakatsuji, H.; Caricato, M.; Li, X.; Hratchian, H. P.; Izmaylov, A. F.; Bloino, J.; Zheng, G.; Sonnenberg, J. L.; Hada, M.; Ehara, M.; Toyota, K.; Fukuda, R.; Hasegawa, J.; Ishida, M.; Nakajima, T.; Honda, Y.; Kitao, O.; Nakai, H.; Vreven, T.; Montgomery, Jr., J. A.; Peralta, J. E.; Ogliaro, F.; Bearpark, M.; Heyd, J. J.; Brothers, E.; Kudin, K. N.; Staroverov, V. N.; Kobayashi, R.; Normand, J.; Raghavachari, K.; Rendell, A.; Burant, J. C.; Iyengar, S. S.; Tomasi, J.; Cossi, M.; Rega, N.; Millam, J. M.; Klene, M.; Knox, J. E.; Cross, J. B.; Bakken, V.; Adamo, C.; Jaramillo, J.; Gomperts, R.; Stratmann, R. E.; Yazyev, O.; Austin, A. J.; Cammi, R.; Pomelli, C.; Ochterski, J. W.; Martin, R. L.; Morokuma, K.; Zakrzewski, V. G.; Voth, G. A.; Salvador, P.; Dannenberg, J. J.; Dapprich, S.; Daniels, A. D.; Farkas, Ö.; Foresman, J. B.; Ortiz, J. V.; Cioslowski, J.; Fox, D. J. *Gaussian 09W*, Version 7.0; Gaussian, Inc.: Wallingford, CT, 2009.

(32) Ghedini, M.; Pucci, D.; Crispini, A.; Barbiero, G. *Organometallics* **1999**, *18*, 2116.

(33) The dinuclear complex **PtIr** would be difficult to synthesize in practice, since all approaches to the preparation of Ir(N^C)2(L^X) complexes rely on the initial, simultaneous introduction of the two N^C coordinating ligands.

(34) Dennington, R. D.; Keith, T. A.; Millam, J. M. *GaussView 5.0.9*; Semichem, Inc: Shawnee, KS, 2000−2008.

(35) Van Houten, J.; Watts, R. J. *J. Am. Chem. Soc.* **1976**, *98*, 4853.

(36) Murov, S. L.; Carmichael, I.; Hug, G. L. *Handbook of Photochemistry*, 2nd ed.; Marcel Dekker: New York, 1993.